Electronic Supplementary Information

Radiation-Hard Organic Electronics with Fullerene-Based Semiconductors

Sergey A. Kuklin,[a] Petr M. Kuznetsov,[a] Valeria S. Bolshakova,[a]Alexander V. Mumyatov,[a] Nikita A. Slesarenko,[a] Galina A. Kichigina,[a] Ivan A. Komarov,[a,b] Pavel P. Kushch,[a] Dmitry P. Kiryukhin,[a] Ivan S. Zhidkov[c,d] and Pavel A. Troshin*[e,a]

[a] *Federal Research Center for Problems of Chemical Physics and Medicinal Chemistry RAS, Academician Semenov ave. 1, Chernogolovka, Moscow region, 142432, Russian Federation*

[b] *Moscow Polytechnical University, B. Semenovskaya st. 38., 107023 Moscow, Russian Federation*

[c] *Institute of Physics and Technology, Ural Federal University, Mira 19 Street, Yekaterinburg, 620002, Russia*

[d] *M. N. Mikheev Institute of Metal Physics of Ural Branch of Russian Academy of Sciences, S. Kovalevskoi 18 Street, Yekaterinburg, 620108, Russia*

[e] *Zhengzhou Advanced Research Institute of HIT, Longyuan East 7th, 26, Jinshui District, 450003 Zhengzhou, China*

Contents:

Experimental Details

1.1. General

All reagents and solvents were obtained from Sigma-Aldrich and Acros Organics and used without further purification. ^{1}H NMR spectra were recorded using Bruker AVANCE-III 500 NMR spectrometer in $CDCl_3$ (δH = 7.27 ppm). MALDI mass spectra (negative ion mode) were acquired using a Bruker Autoflex Speed TOF/TOF device (SmartBeam II laser, 355 nm).

1.2. Device fabrication

The lateral resistor devices were fabricated and characterized as described previously (P. M. Kuznetsov, S. L. Nikitenko, M. V. Zhidkov, D. P. Kirukhin, E. V. Golosov, P. A. Troshin. Mendeleev Commun., 2025, 35, 684). The OFETs were fabricated using the following procedure. Soda lime glass substrates (15x15 mm^2) were mechanically cleaned with water, acetone and toluene, and then treated with air plasma (40 kHz, 300 W) to remove organic contaminants. Then, an aluminum gate electrode (100 nm) was deposited in vacuum at a rate of 3-5 A/s. Next, an AlO_x dielectric layer was formed atop the Al gate surface using anodic oxidation, which was carried out for 10 minutes in a citric acid solution (2.8 g per 50 ml of distilled water) at a voltage of 30 V and a current <100 μA. After anodization, the samples were washed with plenty of clean water and dried in air at a temperature of 60-80°C. Next, 80 nm thick C_{60} semiconductor layer was formed using vacuum deposition at a rate of 1...1.5 A/s. The $PC_{61}BM$ film was spin-coated from 10 mg/ml solution in chlorobenzene (300 rpm for 30 s followed by 2000 rpm for 15s). The device architecture was finalized by thermal evaporation of 100 nm thick Ag source and drain electrodes. The channel length between the electrodes was 40 μm, the width was 1 mm.

1.3. Radiation exposure experiments

The radiation hardness of materials and devices under exposure to gamma rays was studied under anoxic nitrogen or argon atmosphere using Gammatok-100 setup as described previously (V.V. Ozerova, N.A. Emelianov, D.P. Kiryukhin, P.P. Kushch, G.V. Shilov, G.A. Kichigina, S.M. Aldoshin, L.A. Frolova, P.A. Troshin, *J. Phys. Chem. Lett.,* 2023, **14**, 743). The samples were sealed inside the glove box in glass tubes (powders) or multilayer plastic packages under a pure nitrogen atmosphere, excluding exposure of atmospheric air and humidity. The air-tight containers with the samples were exposed to gamma radiation at specific doses of 10, 20, 50, 100, 250, 500, 1000, 2500, etc. kGy (Si) with the dose rate of 1.3 Gy s^{-1} (Si). After exposure, the container was introduced inside the glove box and opened under anoxic conditions for sample characterization. Thus, the contact of the samples with air was completely eliminated within the entire length of the experiment.

1.4. Electrical measurements

The electrical characteristics of the devices were measured using Keithley 2612B 2-channel source-measurement unit inside the glovebox with inert (nitrogen) atmosphere with O_2 and H_2O levels below 1 ppm. The measurements of I-V curves were performed with integration time of 1 NPLC. To perform dynamic photoresponse measurements, 10W white LED was modulated with Advantest TR6240A instrument synchronized with the source-measurement unit collecting the I-V data. Coherent Field Max II-TO instrument with silicon diode OP-2 was used to measure the light intensity.

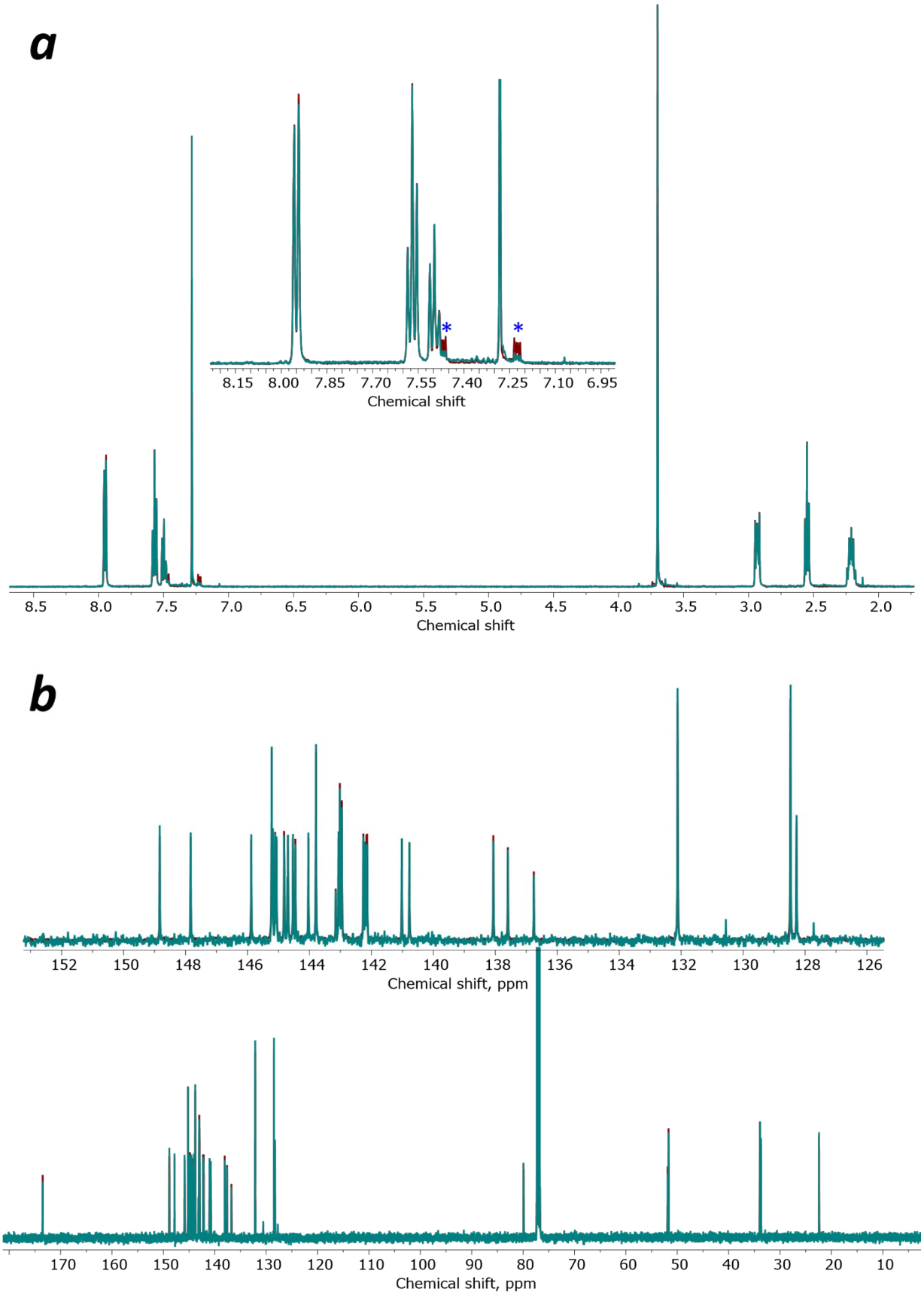

Figure S1. ^{1}H (a) and ^{13}C (b) NMR spectra of $PC_{61}BM$ before (red) and after (cyan) exposure to 8.0 MGy of gamma rays. Symbols "*" denote 1,2-dichlorobenzene solvent impurity.

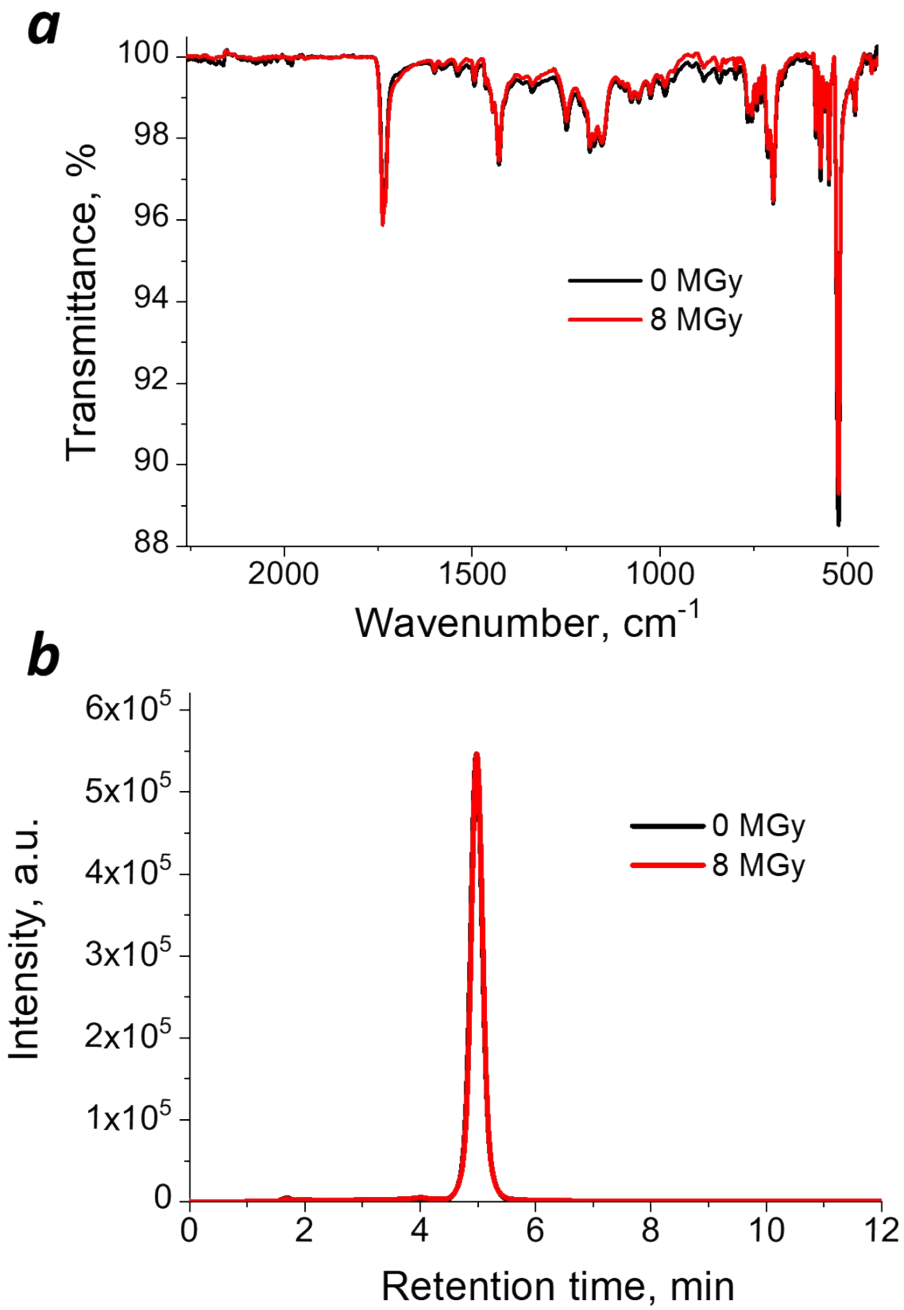

Figure S2. FTIR spectra (a) and HPLC profiles (b) NMR spectra of $PC_{61}BM$ before (black) and after (red) exposure to 8.0 MGy of gamma rays. HPLC profiles were recorded using PERKIN-ELMER PL GEL 5 µm (PL-GEL 5u MIX) 7.5×300 mm column with toluene as eluent, 1 mL min^{-1} flow rate.

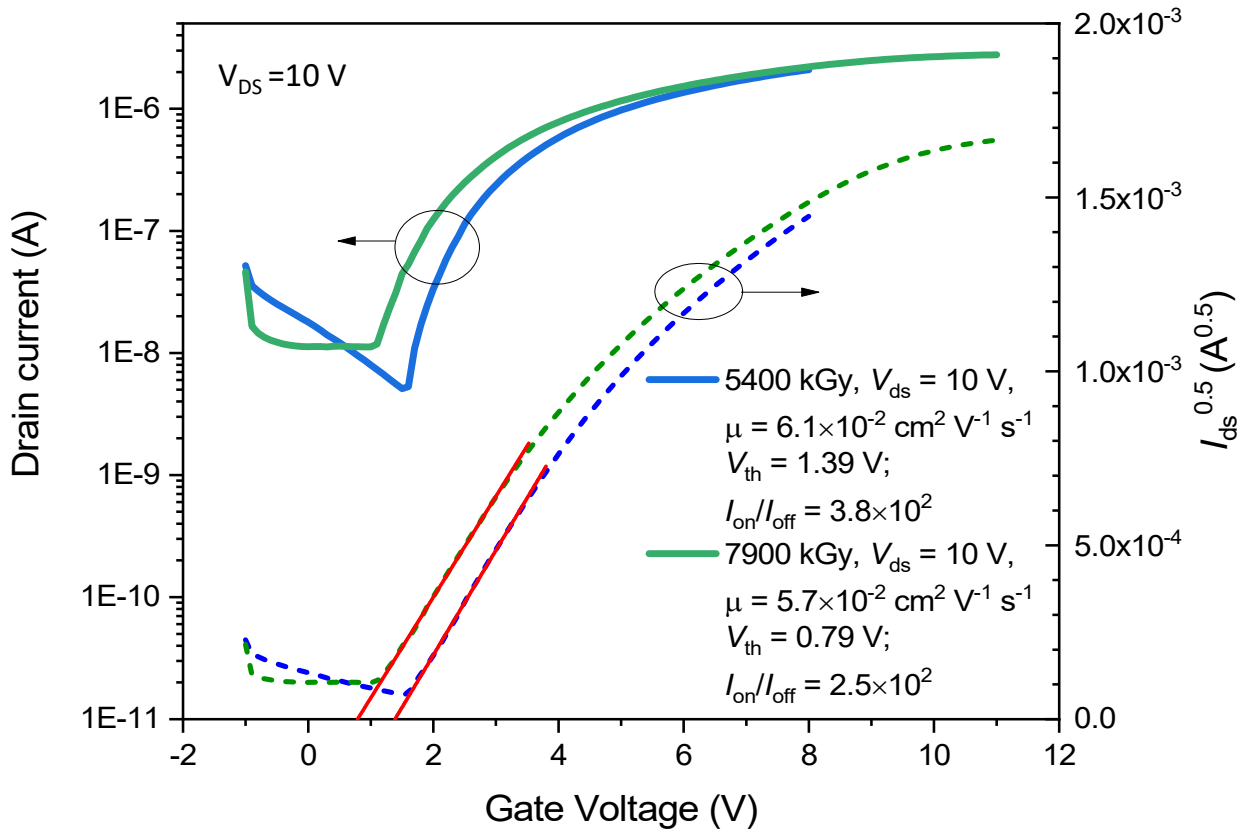

Figure S3. Transfer characteristics and $I_{DS}^{1/2}$ vs. V_{GS} plots for OFETs with $PC_{61}BM$ semiconductor layer after exposure to 5.4 and 7.9 MGy doses of gamma rays.

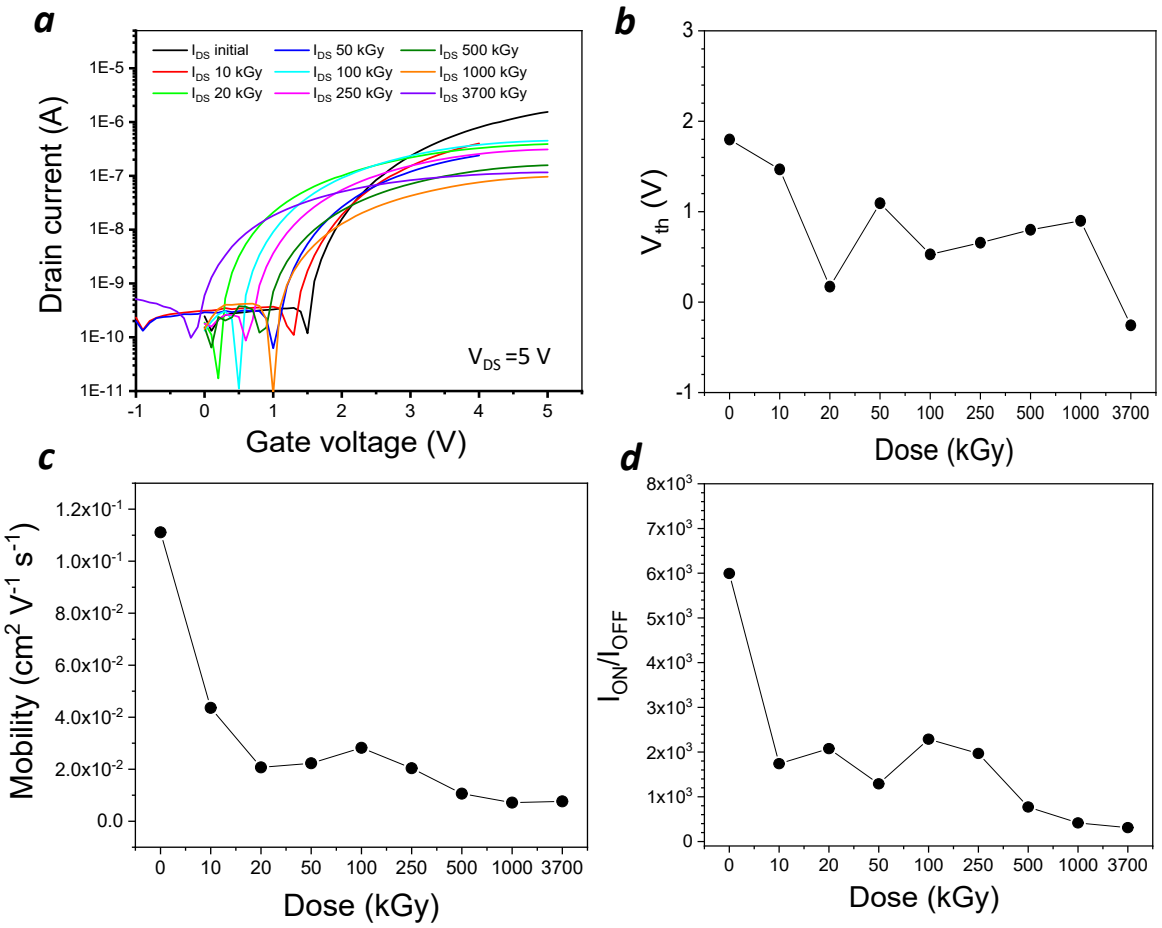

Figure S4. Radiation hardness of C_{60}-based OFETs. Evolution of the device transfer characteristics under radiation exposure (a). Dose-dependent changes in the threshold voltage V_{th} (b), charge carrier mobility (c) and I_{ON}/I_{OFF} ratio (d).

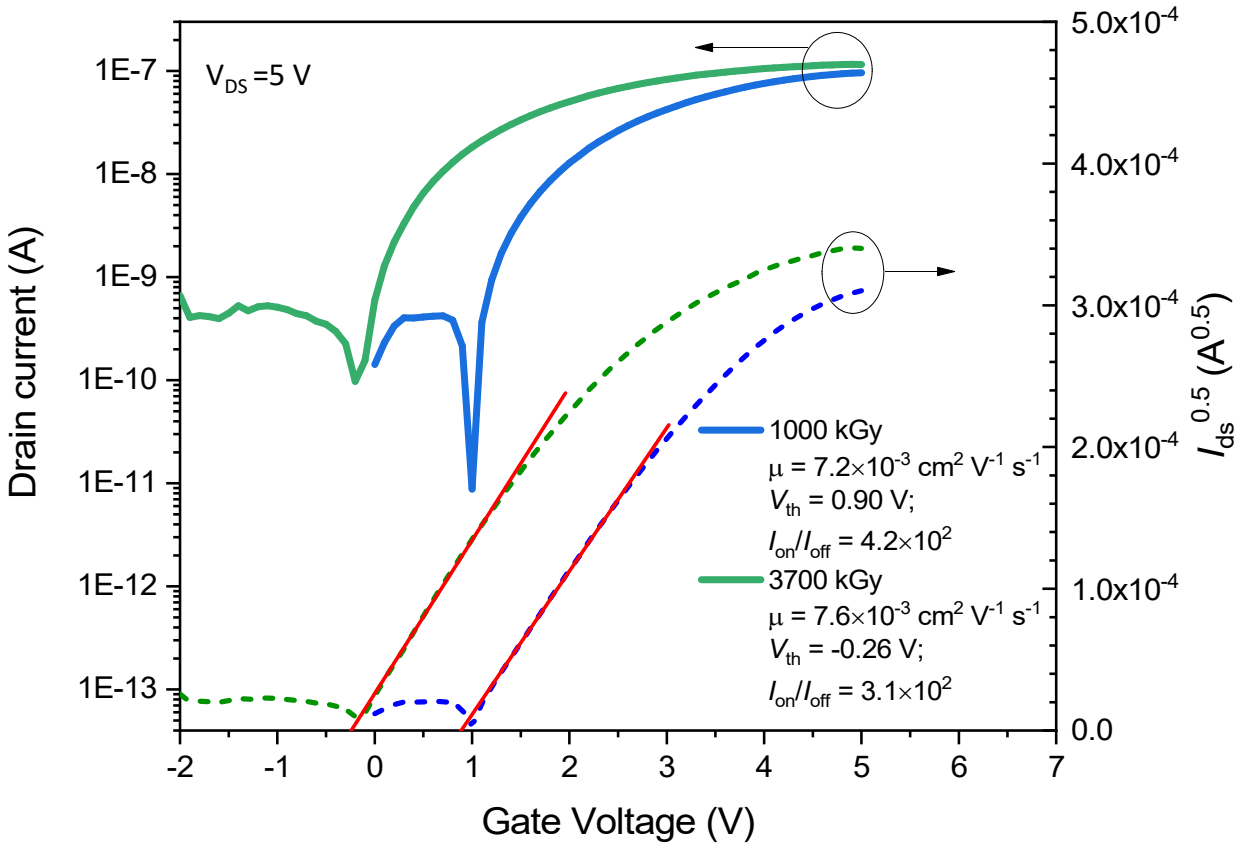

Figure S5. Transfer characteristics and $I_{DS}^{1/2}$ vs. V_{GS} plots for OFETs with C_{60} semiconductor layer after exposure to 1.0 and 3.7 MGy doses of gamma rays.

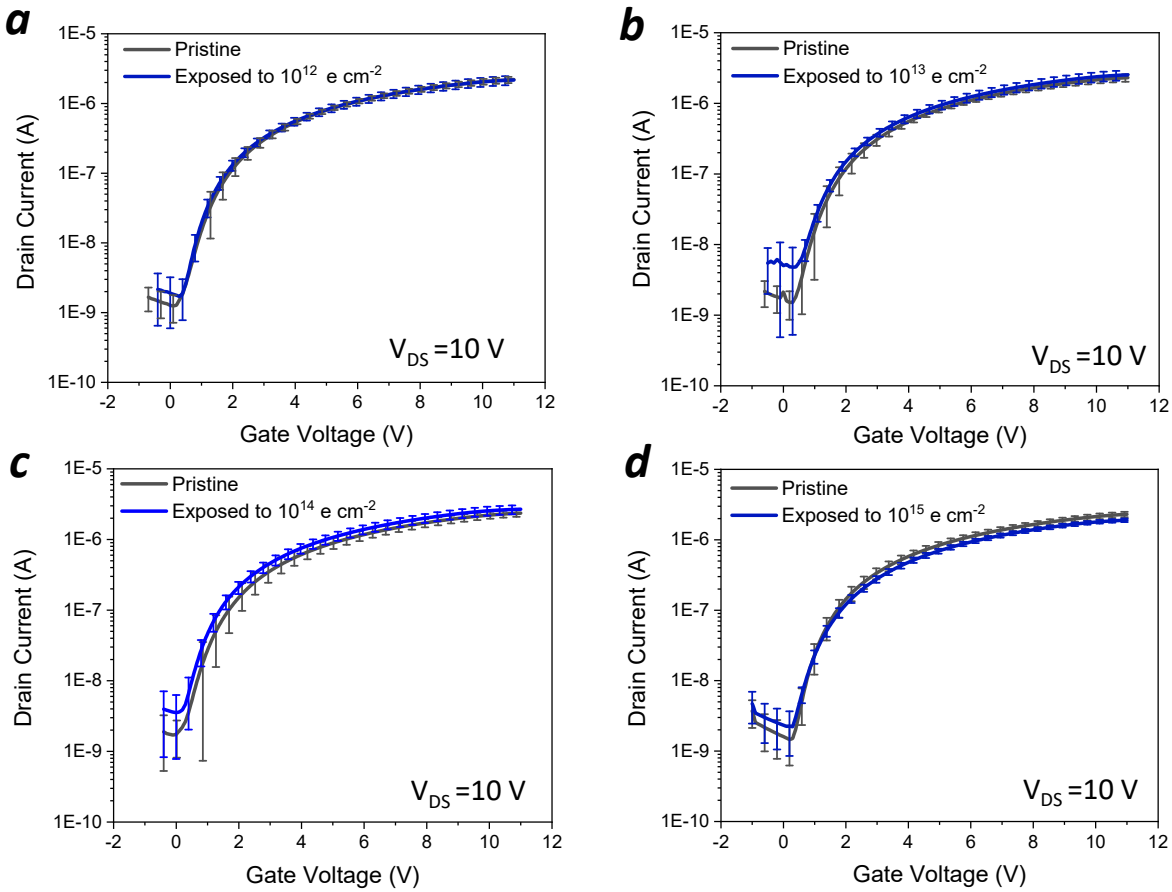

Figure S6. Evolution of the transfer characteristics of $PC_{61}BM$-based OFETs after exposure to different fluences of high-energy electrons: 10^{12} (a), 10^{13} (b), 10^{14} (c) and 10^{15} (d). Statistics was obtained from the batches of at least 20 devices in each group.

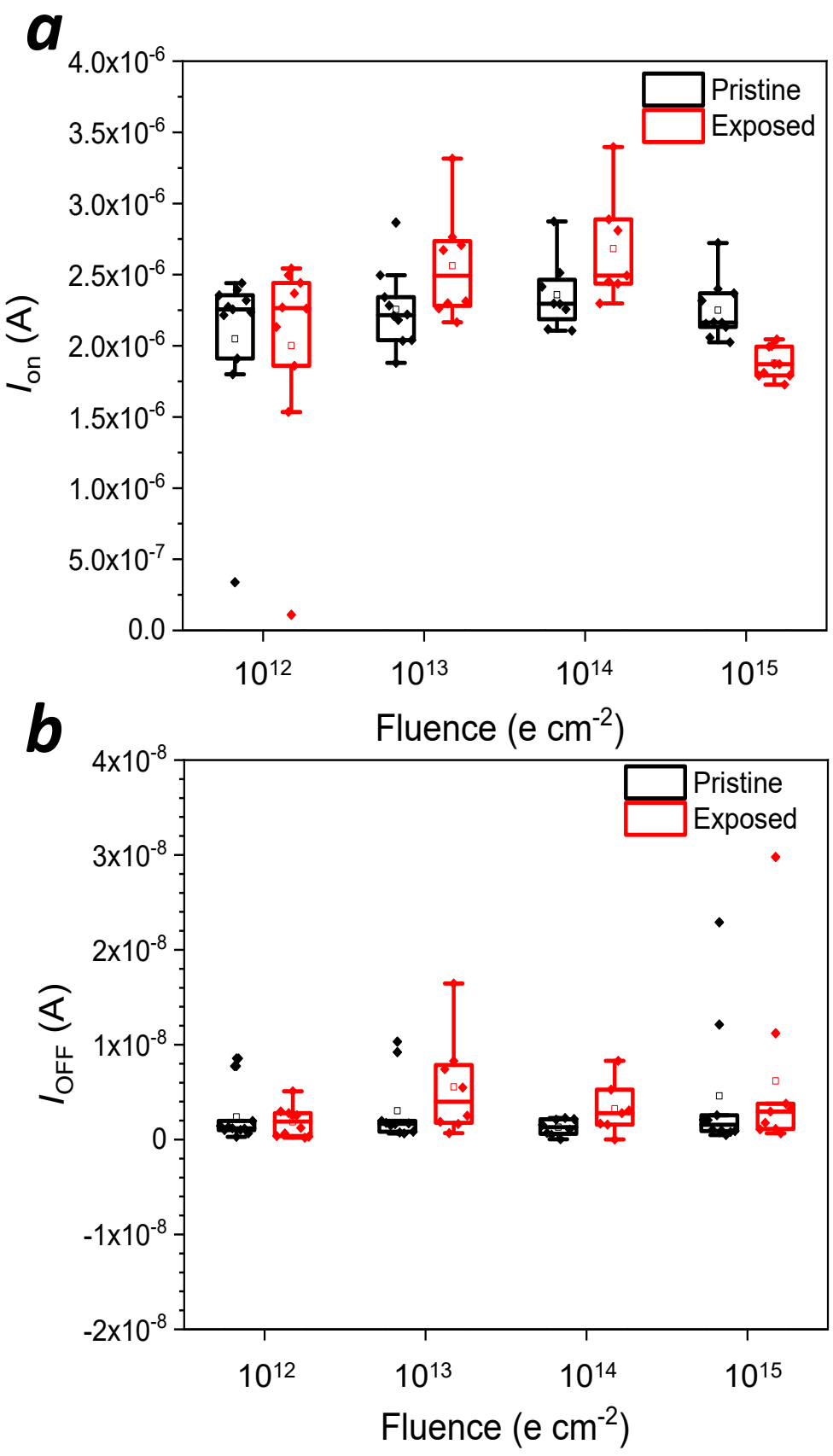

Figure S7. Evolution of the ON (a) and OFF (b) state currents of $PC_{61}BM$-based OFETs after exposure to different fluences of high-energy electrons. Statistics was obtained from the batches of at least 20 devices in each group.

Table S1. Overview of the literature data on the radiation hardness of field-effect transistors based on different semiconductor materials.

Semiconductor material (Device)	**Radiation source**	**Dose or fluence**	**Dose rate**	**Operation voltage $V_{op.}$**	**ΔV_{th}**	**V_{DS}**	**Performance evolution: $\Delta V_{th}/V_{op.}$ or another metric**	**Ref.**
CNTs	^{60}Co γ-rays	40 kGy (Si)	5.6 Gy s^{-1} (Si)	1	0.25	0.25	0.25	1
SWCNTs	^{60}Co γ-rays	10 kGy (Si)	5.3 Gy s^{-1} (Si)	1	0.11	1	0.1	2
CNTs (p-type)	^{60}Co γ-rays	50 kGy (Si)	1.0 Gy s^{-1} (Si)	10	10	1	1	3
CNTs (n-type)				10	3	1.2	0.3	
CNTs (p-type)	^{60}Co γ-rays	60 kGy (Si)	3.0 Gy s^{-1} (Si)	1.5	0.8	2.5	0.53	4
CNTs (n-type)				1.5	0.9	2	0.6	
CNTs (p-type)	^{60}Co γ-rays	30 kGy (Si)	5.6 Gy s^{-1} (Si)	0.8	0.08	0.2	0.1	5
In_2O_3 (n-type)				0.8	0.1	3.2	0.125	
CNTs	^{60}Co γ-rays	22 kGy (Si)	5.6 Gy s^{-1} (Si)	1.5	0.35	1	0.23	6
CNTs	^{60}Co γ-rays	1.5 kGy (Si)	0.5 Gy s^{-1} (Si)	20	4.1	1	0.205	7
CNTs	^{60}Co γ-rays	55 kGy (Si)	1 Gy s^{-1} (Si)	1	0.24	0.25	0.24	8
CNTs	^{60}Co γ-rays	20 kGy (Si)	1.25 Gy s^{-1} (Si)	2	0.9	0.1	0.45	9
SWCNTs	150 keV protons	10^{15} p cm^{-2}	80 nA cm^{-2}	80	20	10	0.25	10
SWCNTs	1 MeV electrons	10^{17} e cm^{-2}	n/a	10	4	0.4	0.4	11
Graphene/hBN	10 keV X-rays	10 kGy (SiO_2)	5.25 Gy s^{-1} (SiO_2)	1.5	n/a	n/a	$\mu/\mu_0 = 0.55$	12
AlGaN/GaN	^{60}Co γ-rays	6 MGy (Si)	5.6 Gy s^{-1} (Si)	3	0.1		0.033	13
InAlN/GaN	^{60}Co γ-rays	6 MGy (Si)	6.54 Gy s^{-1} (Si)	4	0.5		0.125	14
p-GaN	^{60}Co γ-rays	10 kGy (Si)	1 Gy s^{-1} (Si)	2	0.4	1	0.2	15
AlGaN/AlN/GaN	^{60}Co γ-rays	100 kGy (Si)	0.5 Gy s^{-1} (Si)	2	0.4	8	0.2	16
GaN	^{60}Co γ-rays	5 kGy (Si)	0.5 Gy s^{-1} (Si)	5	0.18	100	0.036	17
p-GaN	^{60}Co γ-rays	6 kGy (Si)	0.5 Gy s^{-1} (Si)	3	1.8	0.1	0.6	18
p-GaN	^{60}Co γ-rays	10 kGy (Si)	1 Gy s^{-1} (Si)	2.5	0.55	3	0.22	19
AlGaN	5 MeV protons	10^{14} p cm^{-2}	n/a	6	0.6		0.1	20
MoS_2	2 MeV protons	10^{16} p cm^{-2}	n/a	100	10		0.1	21
MoS_2	200 keV protons	10^{14} p cm^{-2}	n/a	20	2	0.1	0.1	22
In-Zn-O	^{60}Co γ-rays	17 kGy (Si)	0.17 Gy s^{-1} (Si)	20	24	10	1.2	23
Zn-Sn-O	5 MeV protons	10^{15} p cm^{-2}	n/a	40	5	100	0.125	24

Semiconductor material (Device)	**Radiation source**	**Dose or fluence**	**Dose rate**	**Operation voltage $V_{op.}$**	**ΔV_{th}**	**V_{DS}**	**Performance evolution: $\Delta V_{th}/V_{op.}$ or another metric**	**Ref.**
ZnO				40	30	100	0.75	
In-Ga-Zn-O		10^{14} p cm^{-2}		40	100	100	2.5	
In-Ga-Zn-O	^{60}Co γ-rays	5 kGy (Si)	n/a	10	12	0.1	1.2	25
In-W-O	^{60}Co γ-rays	10 kGy (Si)	n/a	20	3.4	10	0.17	26
Zn-In-Sn-O	5 MeV protons	10^{15} p cm^{-2}	n/a	80	5	4	0.062	27
	^{60}Co γ-rays	15 kGy (Si)	4.2 Gy s^{-1} (Si)	80	3.1	4	0.039	
In-Ga-Sn-O	5 MeV protons	10^{13} p cm^{-2}	n/a	20	8	1	0.4	28
In-Ga-Sn-O	3.5 MeV protons	10^{13} p cm^{-2}	n/a	10	6.4	1	0.64	29
In-Ga-Zn-O	x-rays	7 kGy (SiO_2)	1.1 Gy s^{-1} (SiO_2)	20	16	n/a	0.8	30
Zn-Sn-O				20	4	n/a	0.2	
In-Zn-Sn-O				20	2	n/a	0.1	
Zn-In-Sn-O	5 MeV protons	10^{13} p cm^{-2}	n/a	20	0.5	5	0.025	31
SnO_x	50 keV protons	10^{13} p cm^{-2}	n/a	25	16	1	0.64	32
GaInZnO	X-rays 17-19 keV	1 kGy (SiO_2)	0.25 Gy s^{-1} (SiO_2)	5	0		0	33
OFET (Polyera ActivInk)				40	5	60	0.125	
Pentacene OFET	X-rays	2 kGy (SiO_2)	n/a	25	n/a	20	$\mu/\mu_0 = 0.78$	34
OFET	6 MeV X-ray	5 Gy (SiO_2)	0.6 Gy s^{-1} (SiO_2)	40	8	40	0.2	35
OFET (TIPS pentacene)	3 MeV protons	10^{13} p cm^{-2}	n/a	4	>5	2	1.25	36
SiC	^{60}Co γ-rays	6 MGy (Si)	1 Gy s^{-1} (Si)	5	4	10	0.8	37
Si (SOI finFET)	10 keV X-rays	5 kGy (SiO_2)	5.25 Gy s^{-1} (SiO_2)	1	0.06	1	0.06	38
Si p-MOSFET	^{60}Co γ-rays	20 kGy (Si)	n/a	1	4.5	n/a	4.5 (+complete failure)	39
Si n-MOSFET		30 kGy (Si)		1	3	n/a	3 (+complete failure)	
$PC_{61}BM$ OFET	^{60}Co γ-rays	5 MGy (Si)	1.3 Gy s^{-1} (Si)	10	1.5	10	**0.15**	This work
		5 MGy (Si)		10	0.35	10	**0.035***	
		7.9 MGy (Si)		10	1.2	10	**0.12****	
C_{60} OFET		3.7 MGy (Si)		5	2	5	**0.4**	

* excluding the hardening effect of the first small dose of 10 kGy

** individual devices

References

1. M. Zhu, H. Xiao, G. Yan, P. Sun, J. Jiang, Z. Cui, J. Zhao, Z. Zhang and L.-M. Peng, *Nat. Electron.*, 2020, **3**, 622–629.
2. J. J. McMorrow, C. D. Cress, W. A. Gaviria Rojas, M. L. Geier, T. J. Marks and M. C. Hersam, *ACS Nano*, 2017, **11**, 2992–3000.
3. Y. Zhao, D. Li, L. Xiao, J. Liu, X. Xiao, G. Li, Y. Jin, K. Jiang, J. Wang, S. Fan and Q. Li, *Carbon*, 2016, **108**, 363–371.
4. K. Zhang, D. Zhou, N. Gao, J. Zhang, Z. Tong, J. Zhao, P. Liu, X. Wang, X. Lin, H. Xu, L.-M. Peng and W. Zhao, *Sci. Adv.*, 2025, **11**, eadw0024.
5. M. Luo, M. Zhu, M. Wei, S. Shao, M. Robin, C. Wei, Z. Cui, J. Zhao and Z. Zhang, *ACS Appl. Mater. Interfaces*, 2020, **12**, 49963–49970.
6. M. Zhu, Z. Zhang and L. Peng, *Adv. Elect. Materials*, 2019, **5**, 1900313.
7. X. Zhao, M. Yu, L. Cai, J. Liu, J. Wang, H. Wan, J. Wang, C. Wang and Y. Fu, *AIP Advances*, 2019, **9**, 105121.
8. N. Zhang, J. Li, N. Sui, K. Kang, M. Deng, S. Shao, W. Gu, L. Liang, M. Li and J. Zhao, *Nano Lett.*, 2024, **24**, 7688–7697.
9. Y. Liang, Q. Chen, R. Chen, R. Yuan, Z. Wang, H. Yu and J. Han, *IEEE Access*, 2025, **13**, 93941–93948.
10. X. Zhang, H. Zhu, S. Peng, G. Xiong, C. Zhu, X. Huang, S. Cao, J. Zhang, Y. Yan, Y. Yao, D. Zhang, J. Shi, L. Wang, B. Li and Z. Jin, *J. Semicond.*, 2021, **42**, 112002.
11. S. A. Francis, C. D. Cress, J. W. McClory, E. A. Moore and J. C. Petrosky, *IEEE Trans. Nucl. Sci.*, 2013, **60**, 4087–4093.
12. C. X. Zhang, B. Wang, G. X. Duan, E. X. Zhang, D. M. Fleetwood, M. L. Alles, R. D. Schrimpf, A. P. Rooney, E. Khestanova, G. Auton, R. V. Gorbachev, S. J. Haigh and S. T. Pantelides, *IEEE Trans. Nucl. Sci.*, 2014, **61**, 2868–2873.
13. O. Aktas, A. Kuliev, V. Kumar, R. Schwindt, S. Toshkov, D. Costescu, J. Stubbins and I. Adesida, *Solid-State Electronics*, 2004, **48**, 471–475.
14. H.-Y. Kim, J. Kim, L. Liu, C.-F. Lo, F. Ren and S. J. Pearton, *J. Vac. Sci. Technol. B*, 2013, **31**, 051210.
15. Y. Sun, Y. Wang, W. Cui, H. Huang, Y. Song and F. Cao, *Nucl. Eng. Technol.*, 2026, **58**, 103902.
16. Y.-P. Wang, Y.-H. Luo, W. Wang, K.-Y. Zhang, H.-X. Guo, X.-Q. Guo and Y.-M. Wang, *Chinese Phys. C*, 2013, **37**, 056201.
17. H. Wu, X. Fu, J. Guo, T. Liu, Y. Wang, J. Luo, Z. Huang and S. Hu, *IEEE Electron. Device Lett.*, 2022, **43**, 1945–1948.
18. Z. Wang, X. Zhou, Q. Jiang, Z. Peng, H. Wen, Q. Zhou, Z. Qi, M. Qiao, Z. Li and B. Zhang, *IEEE Trans. Electron. Devices*, 2025, **72**, 1002–1007.
19. L. Zhang, Y. Qiu, P. Zhang, Y. Yin, T. Wang and X. Zhou, *Phys. Scr.*, 2024, **99**, 025978.
20. S.-J. Chang, K. J. Cho, H.-W. Jung, J.-J. Kim, Y.-J. Jang, S.-B. Bae, D.-S. Kim, Y. Bae, H. S. Yoon, H.-K. Ahn, B.-G. Min, H. Kim, J.-W. Lim and D.-M. Kang, *ECS J. Solid State Sci. Technol.*, 2019, **8**, Q245–Q248.
21. A. J. Arnold, T. Shi, I. Jovanovic and S. Das, *ACS Appl. Mater. Interfaces*, 2019, **11**, 8391–8399.
22. S. Chen, C. Luo, W. Qin, Z. Yang, T. Liao and C. Jiang, *J. Phys. Chem. C*, 2025, **129**, 16445–16453.
23. A. Indluru, K. E. Holbert and T. L. Alford, *Thin Solid Films*, 2013, **539**, 342–344.
24. B. Park, D. Ho, G. Kwon, D. Kim, S. Y. Seo, C. Kim and M. Kim, *Adv. Funct. Materials*, 2018, **28**, 1802717.
25. G. Yang, G. Huang, H. Zhu, H. Wu, T. Li, T. Huang, Z. Yu, Y. Xu, W. Sun, W. Wu and J. Bi, *IEEE Electron. Device Lett.*, 2025, **46**, 440–443.
26. D.-B. Ruan, P.-T. Liu, K.-J. Gan, Y.-C. Chiu, C.-C. Hsu and S. M. Sze, *Appl. Phys. Lett.*, 2020, **116**, 182104.

27. D. Ho, S. Choi, H. Kang, B. Park, M. N. Le, S. K. Park, M.-G. Kim, C. Kim and A. Facchetti, *ACS Appl. Mater. Interfaces*, 2023, **15**, 33751–33762.
28. M.-G. Shin, S.-H. Hwang, H.-S. Cha, H.-S. Jeong, D.-H. Kim and H.-I. Kwon, *Surf. Interf.*, 2021, **23**, 100990.
29. S.-H. Hwang, K. Yatsu, D.-H. Lee, I.-J. Park and H.-I. Kwon, *Appl. Surf. Sci.*, 2022, **578**, 152096.
30. D. Kang, S. Jeon, E. C. Ju, J. Shin, D. Nam, J. Kim and S. K. Park, *Electron. Mater. Lett.*, DOI:10.1007/s13391-026-00633-8.
31. H. Kang, D. Ho, Y. Kim, J. Kim, H. Kim and C. Kim, *J. Mater. Chem. C*, 2023, **11**, 11542–11551.
32. T. Lv, W. Qin, R. Hong, J. You, Y. Lv, L. Liao and C. Jiang, *ACS Appl. Electron. Mater.*, 2024, **6**, 8748–8756.
33. T. Cramer, A. Sacchetti, M. T. Lobato, P. Barquinha, V. Fischer, M. Benwadih, J. Bablet, E. Fortunato, R. Martins and B. Fraboni, *Adv. Elect. Mater.*, 2016, **2**, 1500489.
34. A. Mitchell, J. A. Posar, J. Cayley, G. York, M. Lerch, A. J. Mozer, I. Píš, E. Magnano, L. Tosti, M. Pedio, A. Syme, I. G. Hill and M. Petasecca, *Adv. Mater.*, 2026, **38**, e08402.
35. D. Dremann, E. J. Kumar, K. J. Thorley, E. Gutiérrez-Fernández, J. D. Ververs, J. D. Bourland, J. E. Anthony, A. R. S. Kandada and O. D. Jurchescu, *Mater. Horiz.*, 2024, **11**, 134–140.
36. L. Basiricò, A. F. Basile, P. Cosseddu, S. Gerardin, T. Cramer, M. Bagatin, A. Ciavatti, A. Paccagnella, A. Bonfiglio and B. Fraboni, *ACS Appl. Mater. Interfaces*, 2017, **9**, 35150–35158.
37. T. Matsuda, T. Yokoseki, S. Mitomo, K. Murata, T. Makino, H. Abe, A. Takeyama, S. Onoda, Y. Tanaka, M. Kandori, T. Yoshie, Y. Hijikata and T. Ohshima, *MSF*, 2016, **858**, 860–863.
38. F. El Mamouni, E. X. Zhang, R. D. Schrimpf, D. M. Fleetwood, R. A. Reed, S. Cristoloveanu and W. Xiong, *IEEE Trans. Nucl. Sci.*, 2009, **56**, 3250–3255.
39. J. Assaf, I. Mdawar and A. Hallak, *Radiat. Eff. Defects Solids*, 2025, 1–17. https://doi.org/10.1080/10420150.2025.2576866